



HAL
open science

Anomalously high abundance of Crocosphaera in the South Pacific Gyre

Mar Benavides, Mathieu Caffin, Solange Duhamel, Rachel Ann Foster, Olivier Grosso, Cécile Guieu, France van Wambeke, Sophie Bonnet

► **To cite this version:**

Mar Benavides, Mathieu Caffin, Solange Duhamel, Rachel Ann Foster, Olivier Grosso, et al.. Anomalously high abundance of Crocosphaera in the South Pacific Gyre. *FEMS Microbiology Letters*, 2022, 369 (1), <10.1093/femsle/fnac039>. <hal-03986953>

HAL Id: hal-03986953

<https://hal.science/hal-03986953v1>

Submitted on 13 Feb 2023

HAL is a multi-disciplinary open access archive for the deposit and dissemination of scientific research documents, whether they are published or not. The documents may come from teaching and research institutions in France or abroad, or from public or private research centers.

L'archive ouverte pluridisciplinaire **HAL**, est destinée au dépôt et à la diffusion de documents scientifiques de niveau recherche, publiés ou non, émanant des établissements d'enseignement et de recherche français ou étrangers, des laboratoires publics ou privés.



HAL Authorization



<http://mc.manuscriptcentral.com/fems>

Anomalously high abundance of *Crocospaera* in the South Pacific Gyre

Journal:	<i>FEMS Microbiology Letters</i>
Manuscript ID	FEMSLE-21-12-0463.R1
Manuscript Type:	Research Letter
Keywords:	Crocospaera, oligotrophic, diazotrophs, cyanobacteria
Please select the most appropriate subject section for your submission from the drop down list. For full Section descriptions please refer to the Author guidelines at https://academic.oup.com/femsle/pages/instructions_for_authors :	Environmental Microbiology and Microbial Ecology (Editor: Tim Daniell)

SCHOLARONE™
Manuscripts

1
2
3 **1 Abstract**
4
5
6 **2**
7

8 3 The unicellular diazotrophic cyanobacterium *Crocospaera* contributes significantly to fixed
9
10 4 nitrogen inputs in the oligotrophic ocean. In the western tropical South Pacific Ocean
11
12 5 (WTSP), these diazotrophs abound thanks to the phosphorus-rich waters provided by the
13
14 6 South Equatorial Current, and iron provided aeolian and subsurface volcanic activity. East of
15
16 7 the WTSP, the South Pacific Gyre (SPG) harbors the most oligotrophic and transparent
17
18 8 waters of the world's oceans, where only heterotrophic diazotrophs have been reported
19
20 9 before. Here in the SPG we detected unexpected accumulation of *Crocospaera* at 50 m
21
22 10 with peak abundances of 5.26×10^5 *nifH* gene copies L⁻¹. The abundance of *Crocospaera*
23
24 11 at 50 m was in the same order of magnitude as those detected westwards in the WTSP and
25
26 12 represented 100% of volumetric N₂ fixation rates. This accumulation at 50 m was likely due
27
28 13 to a deeper penetration of UV light in the clear waters of the SPG being detrimental for
29
30 14 *Crocospaera* growth and N₂ fixation activity.~~the optimal irradiance conditions at this depth.~~
31
32
33
34
35
36
37 15 Nutrient and trace metal addition experiments did not induce any significant changes in **bulk**
38
39 16 N₂ fixation or *Crocospaera* abundance, indicating that this population was not limited by the
40
41 17 resources tested and could develop in high numbers despite the oligotrophic conditions. Our
42
43 18 findings indicate that the distribution of *Crocospaera* can extend into subtropical gyres and
44
45 19 further understanding of their controlling factors is needed.
46
47
48
49
50
51
52
53
54
55
56
57
58
59
60

21 Introduction

22
23 The Western Tropical South Pacific (WTSP) is a recognized hotspot of N₂ fixation activity
24 with an estimated contribution of ~21% to the global fixed nitrogen input (Bonnet *et al.* 2017;
25 Tang *et al.* 2019). In this region, the filamentous and colony-forming *Trichodesmium* and
26 unicellular *Crocospaera* thrive thanks to year-round surface seawater temperatures above
27 25°C, provision of phosphorus-rich waters transported westwards with the South Equatorial
28 Current, and iron (Fe) inputs are predicted from island weathering and hydrothermal inputs
29 along the Tonga-Kermadec volcanic arc (Bonnet *et al.* 2018; Caffin *et al.* 2018; Guieu *et al.*
30 2018; Messié *et al.* 2020). ~~At the boundary between the WTSP and the South Pacific Gyre
31 (SPG) (~170°W longitude) *Trichodesmium* and *Crocospaera* populations decline abruptly
32 due to the lack of sufficient Fe to sustain their growth and N₂ fixation activity, and are
33 outcompeted by heterotrophic diazotrophs such as Gamma A and the unicellular non-
34 photosynthetic cyanobacterial symbiont, UCYN-A (Bonnet *et al.* 2008; Halm *et al.* 2011;
35 Shiozaki *et al.* 2018; Stenegren *et al.* 2018).~~

36
37 *Crocospaera* is a unicellular diazotrophic cyanobacterium widespread in the open ocean
38 (Moisander *et al.* 2010). It can be present as different phenotypes, including the small cell
39 type (<4 µm) and the large cell type (>4 µm), which are known to have different extracellular
40 polysaccharide excretion capabilities (Bench *et al.* 2013) and geographical distributions
41 (Bench *et al.* 2016). While *Crocospaera* and *Trichodesmium* often share the same niche in
42 the open ocean (Stenegren *et al.* 2018), *Crocospaera* differ from *Trichodesmium* in its N₂
43 fixation diel cycle, where *Crocospaera* fixes N₂ at night and *Trichodesmium* during the day
44 (Zehr and Capone 2020). Also these species have different strategies to cope with iron
45 limitation, *Crocospaera* being advantaged by its low size as well as iron reconditioning
46 between day and night times (Saito *et al.* 2011). These diazotrophs also differ in their
47 organic phosphorus uptake capabilities, with *Trichodesmium* being able of using both

1
2
3 48 phosphonates (P-C bonds) and phosphoesters (P-O-C bonds) (Dyhrman *et al.* 2006), while
4
5 49 *Crocospaera* only has genes to process the latter (Dyhrman and Haley 2006).
6
7 50

8
9 51 At the boundary between the WTSP and the South Pacific Gyre (SPG) (~170°W longitude)
10
11 52 *Trichodesmium* and *Crocospaera* populations decline abruptly due to the lack of sufficient
12
13 53 Fe to sustain their growth and N₂ fixation activity, and are outcompeted by heterotrophic
14
15 54 diazotrophs such as Gamma A and the unicellular non-photosynthetic cyanobacterial
16
17 55 symbiont, UCYN-A (Bonnet *et al.* 2008; Halm *et al.* 2011; Shiozaki *et al.* 2018; Stenegren *et*
18
19 56 *al.* 2018).
20
21
22

23 57 During the OUTPACE cruise (Oligotrophic to UITra oligotrophic PACific Experiment, doi:
24
25 58 10.17600/15000900), crossing the WTSP and the western flank of the SPG, (we
26
27 59 unexpectedly detected high abundances of *Crocospaera* in the ultraoligotrophic waters of
28
29 60 the SPG. Intrigued by this accumulation, here we inspect further the vertical distribution of
30
31 61 *Crocospaera*, and the cell-specific N₂ fixation rate and abundance response to nutrient and
32
33 62 trace metal additions in bottle incubations.
34
35
36
37

38 63

40 64 **Materials and methods**

42 65

45 66 *Sampling, hydrographic and chemical variables*

47 67

49 68 Samples were collected between March 23 and 27, 2015 at a station located in the
50
51 69 oligotrophic SPG (18.42°S 166.06°W), during the OUTPACE cruise (Moutin *et al.* 2017). At
52
53 70 this station, six consecutive casts were carried out to study the vertical distribution of the
54
55 71 abundance, N₂ fixation activity and organic/inorganic nutrient limitation of *Crocospaera*
56
57
58
59
60

1
2
3
4 72 (Table S1). ~~The mixed layer depth (MLD) was calculated according to de Boyer Montégut~~
5
6 73 ~~(de Boyer Montégut 2004).~~
7

8 74

9
10 75 Seawater was obtained from thirteen depths in the photic layer (6, 17, 30, 40, 50, 60, 70, 90,
11
12 76 120, 150 and 180 m) using either a regular or trace metal clean (TMC) rosette frame (Table
13
14 77 S1) holding 24 hydrographic bottles (12 L) and sensors for temperature, salinity (SBE
15
16 78 911plus), chlorophyll fluorescence (Wetlabs ECO-AFL/FL, Philomath, Oregon, USA).

17
18 79 Inorganic nutrient concentrations (nitrate plus nitrite —NO_x, and phosphate—here referred to
19
20 80 as dissolved inorganic phosphorus or DIP) were measured by colorimetric methods with a
21
22 81 detection limit of 0.05 µM (Aminot and Kérouel 2007). Dissolved organic carbon (DOC)
23
24 82 concentrations were measured by high-temperature catalytic oxidation as described in
25
26 83 Panagiotopoulos et al. (Panagiotopoulos *et al.* 2019). Dissolved organic phosphorus (DOP)
27
28 84 was measured by a wet oxidation procedure (Pujo-Pay and Raimbault 1994). Dissolved iron
29
30 85 (dFe) concentrations were obtained by flow injection analyses as described in Bonnet and
31
32 86 Guieu (Bonnet and Guieu 2006), and are available from the supplementary material of
33
34 87 Guieu et al. (Guieu *et al.* 2018).
35
36
37
38
39
40
41
42
43

44 88

45 89 *Abundance of diazotrophs*

46 90

47
48 91 *Crocospaera* cells were enumerated and measured from 2.3 L seawater samples filtered
49
50 92 on 2 µm pore size 25 mm diameter polycarbonate membranes and fixed with
51
52 93 paraformaldehyde diluted in filtered seawater (2% final concentration). The samples were
53
54 94 stored at -80°C until enumeration and size measurement using an epifluorescence
55
56 95 microscope (Zeiss Axioplan, Jena, Germany) fitted with a green (510–560 nm) excitation
57
58
59
60

1
2
3 96 filter. They were counted on 40 fields (1.3 mm² per field; 0-2800 *Crocospaera*-like cells per
4
5
6 97 field) scanned and analyzed with the ImageJ1 software. *nifH* gene copy numbers of UCYN-B
7
8 98 (whose closest cultured relative is *Crocospaera watsonii*), UCYN-A1, UCYN-A2,
9
10 99 *Trichodesmium* and the *Richelia* symbionts of diatoms (diatom-diazotroph associations,
11
12
13 100 DDAs): het1, het2 and het3 were enumerated by TaqMan quantitative PCR (qPCR) assays
14
15 101 as described in Stenegren et al. (Stenegren *et al.* 2018). In nutrient amendment experiments
16
17 102 (described below), *Crocospaera* cells were counted by flow cytometry as described in
18
19
20 103 Berthelot et al., (Berthelot *et al.* 2016).
21
22

104

105 *Bulk N₂ fixation rates*

106

107 Bulk N₂ fixation rates were measured from samples collected in four consecutive casts while
108 on station (Table S1). For each profile, triplicate seawater samples were transferred to
109 transparent polycarbonate 4.3 L bottles, closed gas-tight with silicon septa screwcaps, and
110 spiked with 5 mL of ¹⁵N₂ (98.9% atom%, Cambridge isotopes). The ¹⁵N₂ gas batch used did
111 not contain significant concentrations of other nitrogenous compounds labeled with ¹⁵N, as
112 previously confirmed (Dabundo *et al.* 2014; Benavides *et al.* 2015). The samples were
113 incubated in situ for 24 h on a surface-tethered line at the same depths as samplings. Only
114 at the four depths where the abundance of *Crocospaera* was maximal (i.e., 30, 40, 50 and
115 60 m), samples were incubated in shaded on-deck incubators at the irradiance
116 corresponding to each of these depths using neutral density screening adapted to mimic the
117 light intensity at each corresponding sampling depth. Incubations were stopped by vacuum
118 filtration of the samples onto pre-combusted 25 mm GF/F filters and stored at -20°C until
119 analysis. A subsample of 1 L was filtered onto 0.2 µm polycarbonate filters for subsequent
120

1
2
3
4 120 single-cell N₂ fixation analyses (see below). Surface and DCM seawater samples were also
5
6 121 filtered at time zero (not labelled or incubated) to determine the natural isotopic signature of
7
8 122 ambient particulate nitrogen. Bulk particulate nitrogen concentrations and ¹⁵N/¹⁴N ratios were
9
10 123 determined with an elemental analyzer coupled to an isotope ratio mass spectrometer (EA-
11
12 124 IRMS, Integra 2, SerCon Ltd). The accuracy of the instrument was verified every ten
13
14 125 samples using international reference materials IAEA-N-1 and IAEA-310A. The analytical
15
16 126 precision associated with the mass determination averaged 2.8% for particulate organic
17
18 127 nitrogen. The analytical precision associated with ¹⁵N was 0.0010 atom%¹⁵N for a measured
19
20 128 mass of 0.7 μmol N. N₂ fixation rates were calculated with the equations in Montoya et al.
21
22 129 (Montoya *et al.* 1996). The detection limit was 0.035 nmol N L⁻¹ d⁻¹. To avoid an
23
24 130 overestimation of the ¹⁵N₂ gas equilibration time and consequent underestimation of N₂
25
26 131 fixation rates (White *et al.* 2020), we measured the dissolved ¹⁵N enrichment in incubation
27
28 132 bottles using membrane inlet mass spectrometry analyses as previously described (Kana *et*
29
30 133 *al.* 1994; Bonnet *et al.* 2018).

34 134

37 135 *Cell-specific N₂ fixation rates*

38 136

41
42 137 Single-cell rates of *Crocospaera*-like N₂ fixation rates were determined at 30, 40, 50 and 60
43
44 138 m by nanoscale secondary ion mass spectrometry (nanoSIMS 50L). To maximize the
45
46 139 number of cells analyzed in each nanoSIMS image, *Crocospaera*-like cells were sorted
47
48 140 with a Becton Dickinson Influx Mariner flow cytometer (BD Biosciences, Franklin Lakes, NJ)
49
50 141 prior to nanoSIMS analyses as described in Berthelot et al. (Berthelot *et al.* 2016). After
51
52 142 determining the *Crocospaera*-like cluster, the cells were sorted on a 13 mm diameter 0.2
53
54 143 μm pore size polycarbonate membrane and prepared for nanoSIMS analyses as previously
55
56 144 described (Berthelot *et al.* 2016; Bonnet *et al.* 2016). Samples were sputtered prior to
57
58
59
60

1
2
3
4 145 analyses with a current of ~10 pA for at least 2 min. Subsequently, a cesium primary beam
5
6 146 of ~1.3 pA cesium (16 KeV) focused onto a ~100 nm spot diameter region was scanned
7
8 147 across a 256 x 256 or 512 x 512 pixel raster (depending on the image size), with a counting
9
10 148 time of 1 ms per pixel. Mass resolving power was ~8000 to resolved isobaric interferences.
11
12
13 149 Negative secondary ions ($^{12}\text{C}^{14}\text{N}^-$, $^{12}\text{C}^{15}\text{N}^-$) were collected by electron multiplier detectors,
14
15 150 and secondary electrons were also imaged simultaneously. A total of 10 to 50 serial
16
17 151 quantitative secondary ion images were generated and were combined to create the final
18
19 152 image. Between 20 and 100 planes were generated for each cell analyzed. The number of
20
21 153 *Crocospaera*-like cells analyzed with the nanoSIMS ranged between 40 and 80 per
22
23 154 sample.
24
25
26
27
28
29

30 156 The ^{15}N enrichment of target *Crocospaera*-like cells was used to calculate single-cell N_2
31
32 157 fixation rates as previously described (Foster, Szejrenszy and Kuypers 2013; Bonnet *et al.*
33
34 158 2016). The cellular nitrogen content of *Crocospaera* cells (fmol N cell^{-1}) was calculated on
35
36 159 the basis of their diameter, converted to biovolume assuming a spherical shape and
37
38 160 converted to carbon (Verity *et al.* 2012). A C:N ratio of 8.5:1 was used to transform cellular
39
40 161 carbon content to cellular nitrogen content based on sorted *Crocospaera* cells analyzed by
41
42 162 EA-IRMS (see above). The cellular nitrogen content was multiplied by the abundance of
43
44 163 *Crocospaera* cells (determined by microscopy counts) to assess the biomass of the whole
45
46 164 group present in our samples.
47
48
49
50

51 165

52
53 166 *Whole community nutrient amendment experiment*
54
55

56 167
57
58
59
60

1
2
3
4 168 Amendment experiments were performed inside a shipboard clean-air (Class 100)
5
6 169 laboratory container, under strict trace metal clean conditions according to the GEOTRACES
7
8 170 guidelines (www.geotraces.org/images/Cookbook.pdf). Seawater was sampled from 50 m
9
10 171 (where the abundance of *Crocospaera* was maximal) using a trace metal clean Teflon
11
12 172 (PTFE) diaphragm pump connected to plastic tubing and dispensed into detergent and trace
13
14 173 metal grade acid washed 4.3 L transparent polycarbonate bottles.

15
16
17
18 174 ~~Amendment experiments were performed under strict trace metal clean conditions inside a~~
19
20 175 ~~clean container. Seawater was sampled from 50 m (where *Crocospaera* abundance was~~
21
22 176 ~~maximal) using a trace metal clean Teflon pump and dispensed into trace metal grade acid~~
23
24 177 ~~washed 4.3 L transparent polycarbonate bottles. Sets of triplicate bottles~~ received
25
26
27 178 amendments of different nutrients known to limit N₂ fixation ~~in triplicates~~ which included iron
28
29 179 (“Fe”, solution of ferric citrate at 10 nM final concentration), nickel (“Ni” nickel sulfate at 10
30
31 180 nM final concentration), dissolved inorganic phosphorus (“DIP”, suprapur sodium dihydrogen
32
33 181 phosphate at 1 μM final concentration), dissolved organic phosphorus (“DOP”, a mix of
34
35 182 methylphosphonic acid, 2-aminoethylphosphonic acid and fructose 1,6-biphosphate at 1 μM
36
37 183 final concentration) and volcanic ashes from the archipelago of Vanuatu (Ash), and aerosols
38
39 184 (“dust”) collected on board during the OUTPACE cruise (as described in (Guieu *et al.* 2018)).

40
41
42
43
44 185 Incubations were run for 48 h. The response of bulk N₂ fixation rates and *Crocospaera*
45
46 186 abundance to these additions were tested by mass spectrometry and qPCR assays,
47
48 187 respectively, as described above. Primary production rates were measured using 10% ¹³C-
49
50 188 bicarbonate labeling and 24 h incubations as previously described (Berthelot *et al.* 2017).
51
52 189 Heterotrophic bacterial production rates were obtained from tritiated leucine incubations as
53
54 190 detailed in Van Wambeke *et al.* (Van Wambeke *et al.* 2018).
55
56
57
58
59
60

1
2
3
4 192 **Results**
5
6 193

7
8 194 *Hydrological and biogeochemical environment*
9
10 195

11
12
13 196 Hydrological conditions at our sampling stations remained fairly stable along the six
14
15 197 consecutive casts carried out at our sampling station (Fig. 1). Temperature was >29°C from
16
17 198 the surface down to 30 m at the thermocline, decreasing gradually to 19°C at 200 m (Fig.
18
19 199 1a). Salinity was 35.2 from the surface to 30 m and increased to ~36 at 200 m, showing
20
21 200 more variability among casts than temperature (Fig. 1b). The daytime cast (158) showed
22
23 201 slightly higher oxygen and fluorescence levels than night time casts (190 and 018). Oxygen
24
25 202 levels were ~187 mL L⁻¹ between the surface and 30 m, increasing to 200-210 mL L⁻¹
26
27 203 between 40 and 100 m, then decreasing to ~170 mL L⁻¹ at 200 m (Fig. 1c). Fluorescence
28
29 204 profiles depicted a sharp deep chlorophyll maximum (DCM) at 140 m (Fig. 1d). PAR profiles
30
31 205 reflect that the conditions were cloudy during the second cast (cast160). At the surface, PAR
32
33 206 levels reached 250 μmol photons m⁻² s⁻¹, decreasing exponentially with depth (Fig. 1e). The
34
35 207 1% PAR level was located at 175 m.
36
37
38
39
40
41
42
43

44 209 The concentrations of NO_x were <0.05 μM between the surface and 120 m, then increasing
45
46 210 linearly with depth down to 3.5 μM at 175 m (Fig. 1f). The concentrations of DIP were 0.28
47
48 211 μM at the surface, stable at 0.13 - 0.16 μM between 16 and 92 m, gradually increasing back
49
50 212 to ~0.3 μM at 150 m (Fig. 1g). DOC and DOP concentrations showed stable levels at 74 μM
51
52 213 and 0.15 μM, respectively, between the surface and 60 m, decreasing gradually with depth
53
54 214 (Fig. 1h-i). A decrease in DOP concentrations between 0.15 and 0.13 μM was observed at
55
56
57
58
59
60

215 60 m (Fig. 1i). The concentration of dFe was 0.4 nM at the surface and decreasing to ~0.16 -
216 0.2 nM between 50 and 150 m (Fig. 1j).

217

218 *Bulk and cell-specific N₂ fixation rates*

219

220 Bulk N₂ fixation rates ranged between 0.2 and 0.5 ± 0.1 nmol N L⁻¹ d⁻¹ from the surface down
221 to 30 m, increased to 1.3 nmol N L⁻¹ d⁻¹ at 40 m, subsequently peaking at 50 m and reaching
222 a maximum of 2 nmol N L⁻¹ d⁻¹, then decreasing back to 1 nmol N L⁻¹ d⁻¹ at 60 m (Fig. 2a).

223 Cell-specific *Crocospaera*-like N₂ fixation rates were measured at 30, 40, 50 and 60 m
224 depth. Converting cell-specific to volumetric N₂ fixation rates demonstrated that

225 *Crocospaera* was the major active diazotroph, contributing 54 to 100% of bulk N₂ fixation
226 rates. Cell-specific rates were 0.08 ± 0.02 fmol N cell⁻¹ h⁻¹ at the surface and peaked at 2 ±
227 0.2 fmol N cell⁻¹ h⁻¹ at 50 m (Fig. 2b).

228

229 *Abundance of diazotrophs*

230

231 The depth-integrated (down to 120 m) abundance of *Crocospaera* in the SPG station was
232 two to three orders of magnitude higher than observed in previous studies in the South
233 Pacific (Fig. S24). At the SPG station sampled, the average volumetric abundance of UCYN-
234 B cells was 8.9 ± 0.2 × 10⁴ *nifH* gene copies L⁻¹, their maximum abundance being measured
235 at 50 m with 5.3 ± 0.2 × 10⁵ *nifH* gene copies L⁻¹. Epifluorescence microscopy counts
236 showed lower abundances at the surface and 20 m (1.1 - 2.5 × 10² cells L⁻¹), but agreed with
237 qPCR at finding a peak of 2.5 × 10⁵ cells L⁻¹ at 50 m (Fig. 2c). The average cell diameter of
238 the *Crocospaera*-like cells observed under the microscope and subsequently analyzed by

239 nanoSIMS was 3.5 μm (Fig. S32). Other diazotroph groups were enumerated using qPCR.

240 *Trichodesmium*, UCYN-A1 and UCYN-A2 were only detected at 60 m with $3.7 \times 10^2 \pm 2.2 \times$

241 10^2 , $2.9 \pm 0.2 \times 10^4$ and $3.6 \pm 0.2 \times 10^4$ *nifH* gene copies L^{-1} , respectively (data not shown).

242 DDA groups Het-1, Het-2 and Het-3 were not detected.

243

244 *Microbial community response to nutrients and trace metal additions*

245

246 The response of the whole microbial community from 50 m to DIP, DOP, dFe, Ni, ash, or

247 dust addition is shown in Fig. 3a. N_2 fixation and primary production rates were not

248 significantly enhanced by any of the amendments provided (Fig. 3a, one-way ANOVA

249 $p > 0.05$). Heterotrophic bacterial production rates were significantly enhanced by DOP

250 additions (Fig. 3a, 0.9-fold increase, one-way ANOVA Tukey test $p = 0.04$).

251

252 The abundance of UCYN-A1 increased significantly in response to DIP, DOP and ash

253 additions (one-way ANOVA Tukey test $p = 0.05$, 0.03 and 0.02, respectively), but responded

254 negatively to additions of Ni (Fig. 3a). The abundance of *Crocospaera* did not respond to

255 DIP, Fe or Ni amendments, and decreased in DOP, ash and dust amendments. However,

256 none of these differences were statistically significant (Fig. 3a, one-way ANOVA $p = 0.09$).

257 Finally, *Trichodesmium* was only stimulated by DOP additions (1-fold, one-way ANOVA

258 Tukey test $p = 0.02$).

259

260 **Discussion**

261

1
2
3
4 262 Previous studies have reported *Crocospaera* abundances up to 10^7 *nifH* gene copies L⁻¹ in
5
6 263 the North Pacific Subtropical Gyre (Church *et al.* 2005; Bench *et al.* 2016; Wilson *et al.*
7
8 264 2017) and the WTSP (Moisander *et al.* 2010; Bonnet *et al.* 2015). However, previous studies
9
10 265 in ~~the~~ different parts of the SPG have reported low to undetectable *Crocospaera*
11
12 266 ~~abundances~~ (Bonnet *et al.* 2008; Halm *et al.* 2011; Shiozaki *et al.* 2018). Here we report on
13
14 267 an unexpected high abundance of *Crocospaera* peaking at 50 m in the ultraoligotrophic,
15
16 268 ~~Fe-depleted~~ waters of the SPG.
17
18
19
20 269

21
22 270 The vertical distribution of *Crocospaera* at our station in the SPG differed from that
23
24 271 observed in the North Pacific in previous studies. In the North Pacific Subtropical Gyre,
25
26 272 Church *et al.* (Church *et al.* 2005) reported *Crocospaera* abundances of $\sim 10^3$ - 10^4 *nifH* gene
27
28 273 copies L⁻¹ from the surface to the ~~MLD~~mixed layer depth, which was located at ~ 80 m during
29
30 274 their study in the boreal winter. Also at station ALOHA but during the boreal summer season,
31
32 275 Wilson *et al.* (Wilson *et al.* 2017) found a similar vertical distribution but with abundances
33
34 276 equal or higher than 10^6 *nifH* gene copies L⁻¹. Similarly, Bench *et al.* and Shiozaki *et al.*
35
36 277 (Bench *et al.* 2016; Shiozaki *et al.* 2018) reported abundances of 10^5 - 10^7 *nifH* gene copies
37
38 278 L⁻¹ in the upper mixed layer at various sites in the North Pacific Subtropical Gyre and the
39
40 279 WTSP, with a sharp decrease below 50 m. This typical vertical distribution differs from that
41
42 280 observed here, where low abundances of 10^2 *nifH* gene copies L⁻¹ were measured at the
43
44 281 surface, followed by a peak of 2.56×10^5 *nifH* gene copies L⁻¹ at 50 m and a sharp decline
45
46 282 down to the base of the photic zone (Fig. 2a). *Crocospaera* peaked at 50 m and not at the
47
48 283 subsurface as seen in previous studies cited above. ~~This is likely due to the~~The high
49
50 284 irradiance measured in the upper water column layer ($>200 \mu\text{mol m}^{-2} \text{s}^{-1}$; Fig. 1e) typical of
51
52 285 the SPG, recognized as the clearest waters in the world's oceans (Twardowski *et al.* 2007).
53
54
55
56
57
58
59
60

1
2
3
4 286 ~~This irradiance~~ is well above the optimum at which N₂ fixation saturates in *Crocospaera*
5
6 287 (i.e. ~100 μmol m⁻² s⁻¹; (Inomura *et al.* 2019)), explaining their accumulation at deeper levels
7
8 288 in the water column as compared to other regions of the ocean. However, the cell-specific N₂
9
10 289 fixation peak observed here at 50 m corresponds to ~80 μmol m⁻² s⁻¹ PAR (Fig. 1e), which
11
12 290 would be suboptimal for *Crocospaera* (Inomura *et al.* 2019) and does not explain their
13
14 291 accumulation at this depth. Growth, N₂ and carbon fixation are negatively affected by UV
15
16 292 radiation in cultures of *Crocospaera* (Zhu *et al.* 2020). While no UV data is available for our
17
18 293 cruise, previous studies have found a deeper penetration of UV in the clear waters of the
19
20 294 SPG as compared to other ocean regions (Morel *et al.*, 2007). This could explain why
21
22 295 *Crocospaera* accumulated deeper in the water column during our study (Fig. 2) as
23
24 296 compared to shallower previous observations in other open ocean regions (Church *et al.*
25
26 297 2005; Wilson *et al.* 2017; Stenegren *et al.* 2018; Moisander *et al.* 2010).
27
28
29
30
31

32 298
33
34 299 Previous studies have detected two subpopulations of *Crocospaera* in the South Pacific:
35
36 300 large type (>4 μm) and small type (<4 μm) (Bench *et al.* 2016). Genome comparisons of
37
38 301 several *Crocospaera* strains have shown that while being very similar at the genome level,
39
40 302 strains differ widely in their phenotype and strategies to cope with nutrient and trace metal
41
42 303 stress (Webb *et al.* 2009). The large type harbors more DOP scavenging and iron stress
43
44 304 response genes than the small type (Dyhrman and Haley 2006; Bench *et al.* 2013). The
45
46 305 *Crocospaera* cells observed here belonged to the small type (~3.5 μm) (Fig. S32) and
47
48 306 peaked at 50 m, coinciding with the lowest dFe concentrations measured during our cruise
49
50 307 (0.16 nM, Fig. 1j) (Guieu *et al.* 2018). While these dFe concentrations are limiting for
51
52 308 phytoplankton growth in the SPG (Behrenfeld and Kolber 1999), recent *Crocospaera* cell-
53
54 309 specific dFe uptake rates measured in the same region (0.46 - 1.21 amol Fe cell⁻¹ d⁻¹)
55
56
57
58
59
60

1
2
3
4 310 confirm that this diazotroph is well adapted to thrive in dFe-limited environments (Lory et al.
5
6 311 in rev.). Alternatively, the ~2-3°C temperature increase between 50 m and the on-deck
7
8 312 incubators may have alleviated Fe limitation in *Crocosphaera* (Yang et al. 2021).
9
10 313
11
12
13 314 The peak of *Crocosphaera* at 50 m also coincided with a decrease in DIP concentrations at
14
15 315 50 - 60 m (Fig. 1g), while DOP concentrations did not seem to be variable (Fig. 1h) as
16
17
18 316 compared to the surface. This could be expected in a small *Crocosphaera* cell type
19
20 317 population, less genetically equipped to scavenge DOP than the large cell type (Bench et al.
21
22 318 2013). The locally available concentrations of dFe and DIP seemed to be sufficient to fulfill
23
24 319 the needs of this *Crocosphaera* population, since responses to either dFe or DIP additions
25
26 320 were not observed (Fig. 3b).
27
28
29 321
30
31 322
32
33
34 323 West of the SPG along the OUTPACE cruise transect, *Crocosphaera* abundances peaked at
35
36 324 $10^4 - 10^5$ *nifH* gene copies L⁻¹ at 40 m, in the region where dFe concentrations were highest,
37
38 325 i.e. between 175°E and ~175°W (Guieu et al. 2018). In this region, specific *Crocosphaera*-
39
40 326 like N₂ fixation rates were 0.5 - 2.5 fmol N cell⁻¹ h⁻¹, only contributing 6 to - 10% to bulk N₂
41
42 327 fixation rates (Bonnet et al. 2018). At the SPG station, *Crocosphaera* cell-specific N₂ fixation
43
44 328 ranged between 0.7 and 1.4 fmol N cell⁻¹ h⁻¹, representing 100% of bulk N₂ fixation rates at
45
46 329 all depths except at 30 m (Fig. 2c). These rates are in good agreement with previous
47
48
49 330 *Crocosphaera*-like cell-specific N₂ fixation measurements in the North Pacific Subtropical
50
51 331 Gyre (between 0.1 and 1.1 fmol N cell⁻¹ h⁻¹; (Foster, Szejnrenszus and Kuypers 2013)) and
52
53 332 the WTSP (2.1 fmol N cell⁻¹ h⁻¹; (Berthelot et al. 2016)). Similar cell-specific rates have been
54
55 333 reported for other widespread diazotrophs such as *Trichodesmium* (2.3 fmol N cell⁻¹ h⁻¹;
56
57
58
59
60

334 (Berthelot *et al.* 2016)) and UCYN-A1 (~1 fmol N cell⁻¹ h⁻¹; (Martínez-Pérez *et al.* 2016)),
335 reinforcing the good health and important diazotrophic activity of *Crocospaera* in the SPG
336 during this study.

337

338 Overall, the high abundance, N₂ fixation activity and lack of response to any nutrient or trace
339 metal additions of *Crocospaera* observed in the SPG station indicate that this population
340 was healthy, active, and largely contributing to fixed nitrogen inputs in this ultraoligotrophic
341 environment. In light of the predicted expansion of subtropical gyres (Polovina, Howell and
342 Abecassis 2008), our results suggest that the possibly overlooked abundance and
343 distribution of low-nutrient adapted *Crocospaera* in the SPG deserves further study.

344

345 **Author contribution statement**

346

347 All authors contributed to the sampling and experiments carried out onboard. MC performed
348 microscopy cell counts and nanoSIMS analyses. SD performed ¹⁴C uptake analyses. OG
349 performed IRMS and MIMS analyses. FVW performed heterotrophic bacterial production
350 analyses. MB wrote the paper with contributions from all authors.

351

352 **Competing Interests statement:** The authors declare no competing financial interests.

353

354 **References**

355

356 Aminot A, Kérouel R. *Dosage Automatique Des Nutriments Dans Les Eaux Marines:*

357 *Méthodes En Flux Continu.* Editions Quae, 2007:188.

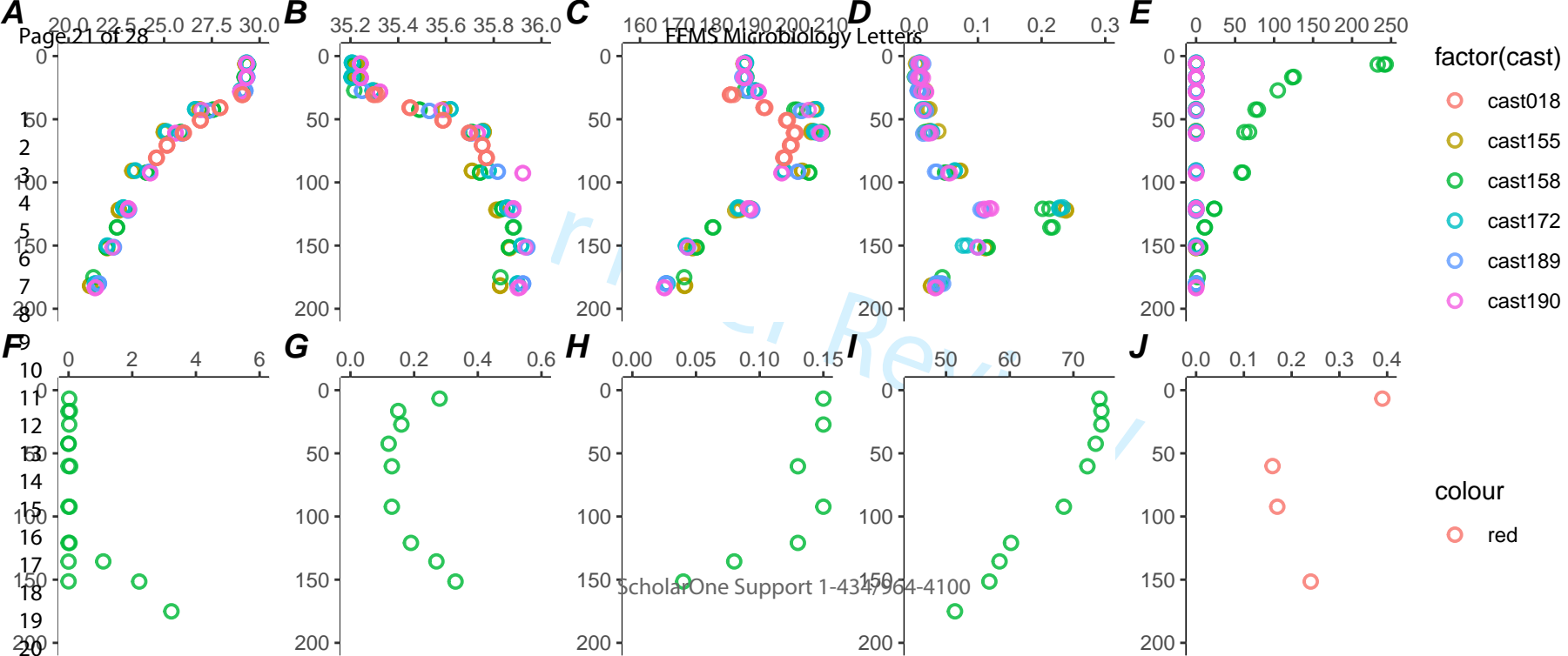
- 1
2
3 358 Behrenfeld MJ, Kolber ZS. Widespread iron limitation of phytoplankton in the south pacific
4
5
6 359 ocean. *Science* 1999;**283**:840–3.
7
- 8 360 Benavides M, Moisander PH, Berthelot H *et al.* Mesopelagic N₂ fixation related to organic
9
10 361 matter composition in the Solomon and Bismarck Seas (Southwest Pacific). *PLoS*
11
12 362 *One* 2015;**10**:1–19.
13
14
- 15 363 Bench SR, Frank I, Robidart J *et al.* Two subpopulations of *Crocospaera watsonii* have
16
17 364 distinct distributions in the North and South Pacific. *Environ Microbiol* 2016;**18**:514–
18
19 365 24.
20
21
- 22 366 Bench SR, Heller P, Frank I *et al.* Whole genome comparison of six *Crocospaera watsonii*
23
24 367 strains with differing phenotypes. *J Phycol* 2013;**49**:786–801.
25
26
- 27 368 Berthelot H, Benavides M, Moisander PH *et al.* High-nitrogen fixation rates in the particulate
28
29 369 and dissolved pools in the Western Tropical Pacific (Solomon and Bismarck Seas).
30
31 370 *Geophys Res Lett* 2017;**44**:8414–23.
32
33
- 34 371 Berthelot H, Bonnet S, Grosso O *et al.* Transfer of diazotroph-derived nitrogen towards non-
35
36 372 diazotrophic planktonic communities: A comparative study between *Trichodesmium*
37
38 373 *erythraeum* *Crocospaera watsonii* and *Cyanothece* sp. *Biogeosciences*
39
40 374 2016;**13**:4005–21.
41
42
43
- 44 375 Bonnet S, Berthelot H, Turk-Kubo K *et al.* Diazotroph derived nitrogen supports diatom
45
46 376 growth in the South West Pacific: A quantitative study using nanoSIMS. *Limnol*
47
48 377 *Oceanogr* 2016, DOI: 10.1002/lno.10300.
49
50
- 51 378 Bonnet S, Caffin M, Berthelot H *et al.* Hot spot of N₂ fixation in the western tropical South
52
53 379 Pacific pleads for a spatial decoupling between N₂ fixation and denitrification.
54
55 380 *Proceedings of the National Academy of Sciences* 2017, DOI:
56
57 381 10.1073/pnas.1619514114.
58
59
60

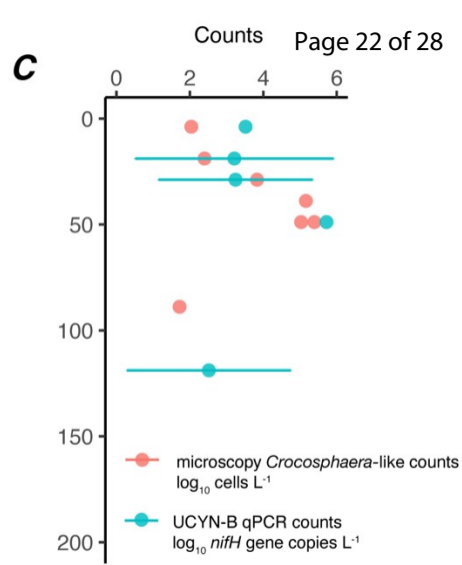
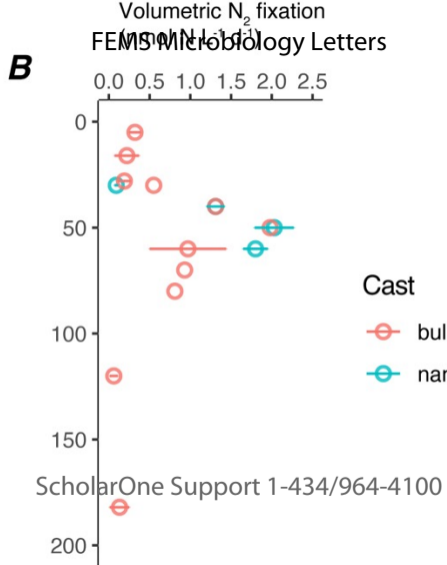
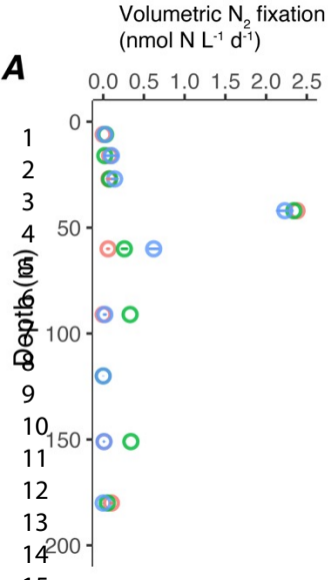
- 1
2
3
4 382 Bonnet S, Caffin M, Berthelot H *et al.* In-depth characterization of diazotroph activity across
5
6 383 the western tropical South Pacific hotspot of N₂ fixation (OUTPACE cruise).
7
8 384 *Biogeosciences* 2018;**15**:4215–32.
- 9
10 385 Bonnet S, Guieu C. Atmospheric forcing on the annual iron cycle in the western
11
12 386 Mediterranean Sea: A 1-year survey. *J Geophys Res* 2006;**111**, DOI:
13
14 387 10.1029/2005jc003213.
- 15
16
17 388 Bonnet S, Guieu C, Bruyant F *et al.* *Nutrient Limitation of Primary Productivity in the*
18
19 389 *Southeast Pacific (BIOCOPE Cruise)*., 2008:215–25.
- 20
21
22 390 Bonnet S, Rodier M, Turk-Kubo KA *et al.* Contrasted geographical distribution of N₂ fixation
23
24 391 rates and nifH phylotypes in the Coral and Solomon Seas (southwestern Pacific)
25
26 392 during austral winter conditions. *Global Biogeochem Cycles* 2015;**29**:1874–92.
- 27
28
29 393 Caffin M, Moutin T, Ann Foster R *et al.* N₂ fixation as a dominant new N source in the
30
31 394 western tropical South Pacific Ocean (OUTPACE cruise). *Biogeosciences* 2018,
32
33 395 DOI: 10.5194/bg-15-2565-2018.
- 34
35
36 396 Church MJ, Jenkins BD, Karl DM *et al.* Vertical distributions of nitrogen-fixing phylotypes at
37
38 397 Stn ALOHA in the oligotrophic North Pacific Ocean. *Aquat Microb Ecol* 2005;**38**:3–14.
- 39
40
41 398 Dabundo R, Lehmann MF, Treibergs L *et al.* The contamination of commercial 15N₂ gas
42
43 399 stocks with 15N-labeled nitrate and ammonium and consequences for nitrogen
44
45 400 fixation measurements. *PLoS One* 2014;**9**, DOI: 10.1371/journal.pone.0110335.
- 46
47
48 401 Dyhrman ST, Chappell PD, Haley ST *et al.* Phosphonate utilization by the globally important
49
50 402 marine diazotroph *Trichodesmium*. *Nature* 2006;**439**:68–71.
- 51
52
53 403 Dyhrman ST, Haley ST. Phosphorus scavenging in the unicellular marine diazotroph
54
55 404 *Crocospaera watsonii*. *Appl Environ Microbiol* 2006;**72**:1452–8.
- 56
57
58
59
60

- 1
2
3
4 405 Foster RA, Sztejnusz S, Kuypers MMM. Measuring carbon and N₂ fixation in field
5
6 406 populations of colonial and free-living unicellular cyanobacteria using nanometer-
7
8 407 scale secondary ion mass spectrometry. *J Phycol* 2013;**49**:502–16.
9
10 408 Guieu C, Bonnet S, Petrenko A *et al.* Iron from a submarine source impacts the productive
11
12 409 layer of the Western Tropical South Pacific (WTSP). *Sci Rep* 2018;**8**:9075.
13
14
15 410 Halm H, Lam P, Ferdelman TG *et al.* Heterotrophic organisms dominate nitrogen fixation in
16
17 411 the South Pacific Gyre. *ISME J* 2011;**6**:1238–49.
18
19
20 412 Inomura K, Deutsch C, Wilson ST *et al.* Quantifying Oxygen Management and Temperature
21
22 413 and Light Dependencies of Nitrogen Fixation by *Crocospaera watsonii*. *MSphere*
23
24 414 2019;**4**:1–15.
25
26
27 415 Kana TM, Darkangelo C, Hunt MD *et al.* Membrane Inlet Mass Spectrometer for Rapid
28
29 416 Environmental Water Samples. *Anal Chem* 1994;**66**:4166–70.
30
31
32 417 Martínez-Pérez C, Mohr W, Löscher CR *et al.* The small unicellular diazotrophic symbiont,
33
34 418 UCYN-A, is a key player in the marine nitrogen cycle. *Nature Microbiology* 2016,
35
36 419 DOI: 10.1038/nmicrobiol.2016.163.
37
38
39 420 Messié M, Petrenko A, Doglioli AM *et al.* The Delayed Island Mass Effect: how islands can
40
41 421 remotely trigger blooms in the oligotrophic ocean. *Geophys Res Lett* 2020:1–14.
42
43
44 422 Moisander PH, Beinart RA, Hewson I *et al.* Unicellular cyanobacterial distributions broaden
45
46 423 the oceanic N₂ fixation domain. *Science* 2010;**327**:1512–4.
47
48
49 424 Montoya JP, Voss M, Kahler P *et al.* A Simple, High-Precision, High-Sensitivity Tracer Assay
50
51 425 for N₂ Fixation. *Appl Environ Microbiol* 1996;**62**:986–93.
52
53
54 426 Moutin T, Michelangelo Doglioli A, De Verneil A *et al.* Preface: The Oligotrophy to the Uitra-
55
56 427 oligotrophy PACific Experiment (OUTPACE cruise, 18 February to 3 April 2015).
57
58 428 *Biogeosciences* 2017, DOI: 10.5194/bg-14-3207-2017.
59
60

- 1
2
3
4 429 Panagiotopoulos C, Pujo-Pay M, Benavides M *et al.* The composition and distribution of
5
6 430 semi-labile dissolved organic matter across the southwest Pacific. *Biogeosciences*
7
8 431 2019;**16**, DOI: 10.5194/bg-16-105-2019.
9
10 432 Polovina JJ, Howell EA, Abecassis M. Ocean's least productive waters are expanding.
11
12
13 433 *Geophys Res Lett* 2008;**35**:2–6.
14
15 434 Pujo-Pay M, Raimbault P. Improvement of the wet oxidation procedure for simultaneous
16
17 435 determination of particulate organic Nitrogen and Phosphorus collected on filters.
18
19
20 436 *Mar Ecol Prog Ser* 1994;**105**:203–7.
21
22 437 Saito MA, Bertrand EM, Dutkiewicz S *et al.* Iron conservation by reduction of metalloenzyme
23
24 438 inventories in the marine diazotroph *Crocospaera watsonii*. *Proc Natl Acad Sci U S*
25
26 439 *A* 2011;**108**:2184–9.
27
28
29 440 Shiozaki T, Bombar D, Riemann L *et al.* Linkage Between Dinitrogen Fixation and Primary
30
31 441 Production in the Oligotrophic South Pacific Ocean. *Global Biogeochem Cycles*
32
33 442 2018;**32**:1028–44.
34
35
36 443 Stenegren M, Caputo A, Berg C *et al.* Distribution and drivers of symbiotic and free-living
37
38 444 diazotrophic cyanobacteria in the western tropical South Pacific. *Biogeosciences*
39
40 445 2018;**15**:1559–78.
41
42
43 446 Tang W, Wang S, Fonseca-Batista D *et al.* Revisiting the distribution of oceanic N₂ fixation
44
45 447 and estimating diazotrophic contribution to marine production. *Nat Commun*
46
47 448 2019;**10**:1–10.
48
49
50 449 Twardowski MS, Claustre H, Freeman SA *et al.* Optical backscattering properties of the
51
52 450 “clearest” natural waters. *Biogeosciences* 2007;**4**:1041–58.
53
54
55
56
57
58
59
60

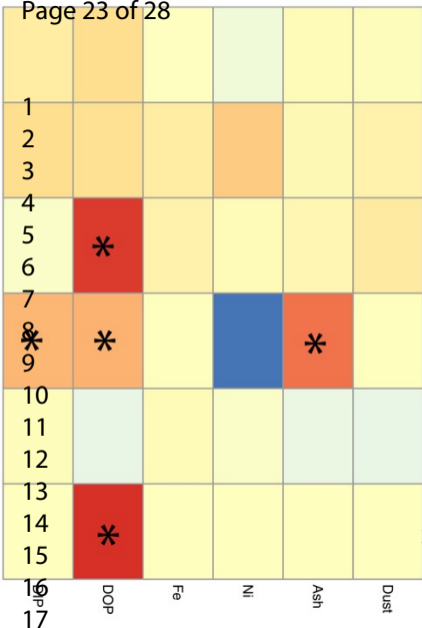
- 1
2
3
4 451 Van Wambeke F, Gimenez A, Duhamel S *et al.* Dynamics and controls of heterotrophic
5
6 452 prokaryotic production in the western tropical South Pacific Ocean: Links with
7
8 453 diazotrophic and photosynthetic activity. *Biogeosciences* 2018;**15**:2669–89.
9
10 454 Verity PG, Robertson CY, Tronzo CR *et al.* Relationships between cell volume and the
11
12 455 carbon and nitrogen content of marine photosynthetic nanoplankton. 2012;**37**:1434–
13
14 456 46.
15
16
17 457 Webb EA, Ehrenreich IM, Brown SL *et al.* Phenotypic and genotypic characterization of
18
19 458 multiple strains of the diazotrophic cyanobacterium, *Crocospaera watsonii*, isolated
20
21 459 from the open ocean. *Environ Microbiol* 2009;**11**:338–48.
22
23
24 460 White AE, Granger J, Selden C *et al.* A critical review of the $^{15}\text{N}_2$ tracer method to measure
25
26 461 diazotrophic production in pelagic ecosystems. *Limnol Oceanogr Methods*
27
28 462 2020;**18**:129–47.
29
30
31 463 Wilson ST, Aylward FO, Ribalet F *et al.* Coordinated regulation of growth, activity and
32
33 464 transcription in natural populations of the unicellular nitrogen-fixing cyanobacterium
34
35 465 *Crocospaera*. *Nature Microbiology* 2017;**2**:1–27.
36
37
38 466 Yang N, Merkel CA, Lin Y-A *et al.* Warming Iron-Limited Oceans Enhance Nitrogen Fixation
39
40 467 and Drive Biogeographic Specialization of the Globally Important Cyanobacterium
41
42 468 *Crocospaera*. *Frontiers in Marine Science* 2021;**8**:118.
43
44
45 469 Zehr JP, Capone DG. Changing perspectives in marine nitrogen fixation. *Science*
46
47 470 2020;**368**:eaay9514.
48
49
50
51
52
53
54
55
56
57
58
59
60



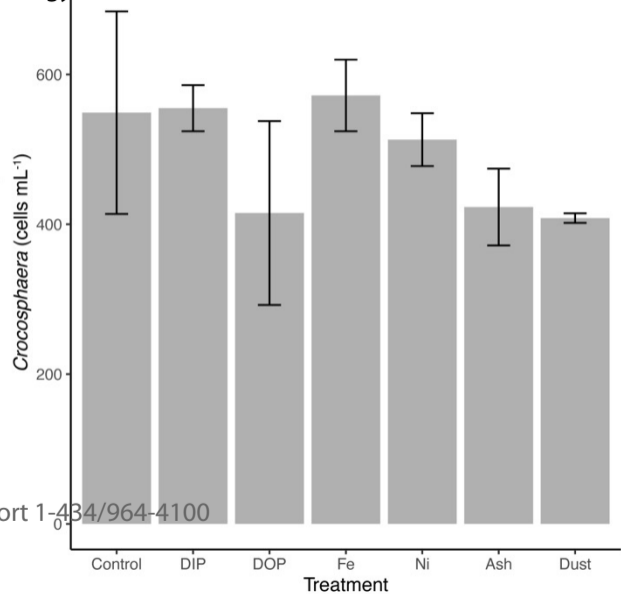


A

Page 23 of 28

**B**

FEMS Microbiology Letters



ScholarOne Support 1-434/964-4100

Supplementary Information

Supplementary figures and tables

Figure S1: Chlorophyll a versus phycoerythrin cytogram showing gating of *Crocospaera* cells prior to sorting for nanoSIMS analyses.

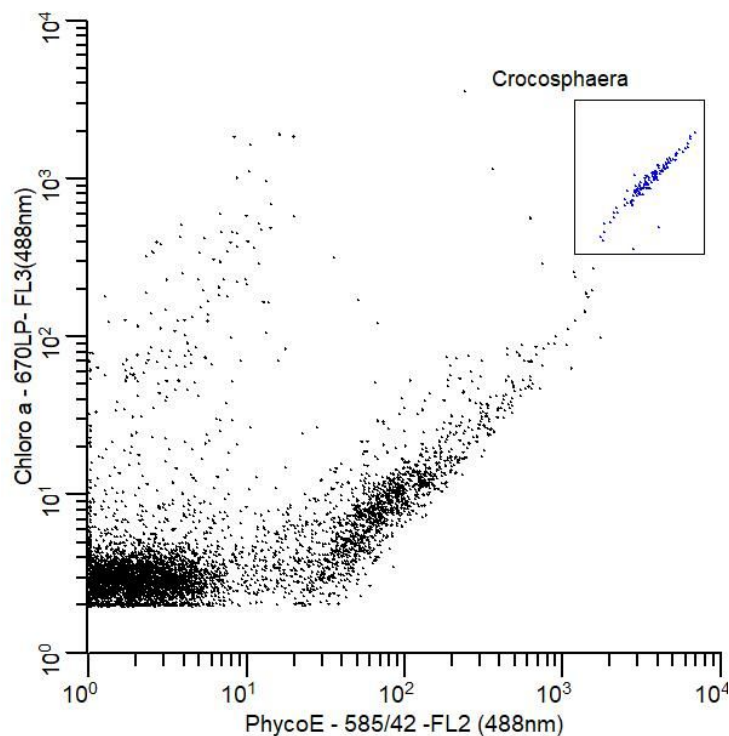


Figure S2: Upper panel: Western Tropical South Pacific map highlighting the region zoomed-in zone in the lower panel. Lower panel: distribution of UCYN-B in the WTSP based on previous publications (data compilation in (Tang *et al.* 2019) and the abundance measured in this study (highest abundance dark red bubble). The maximum integration depths are 120 m and 215 m in this and Tang *et al.* (Tang *et al.* 2019) studies, respectively.

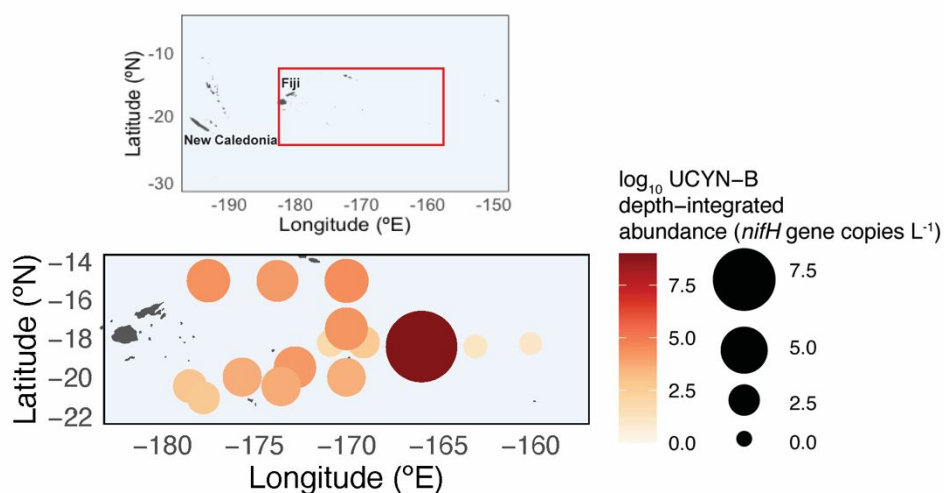


Figure S3: Example of NanoSIMS images of *Crocospaera* cells analyzed during this study.

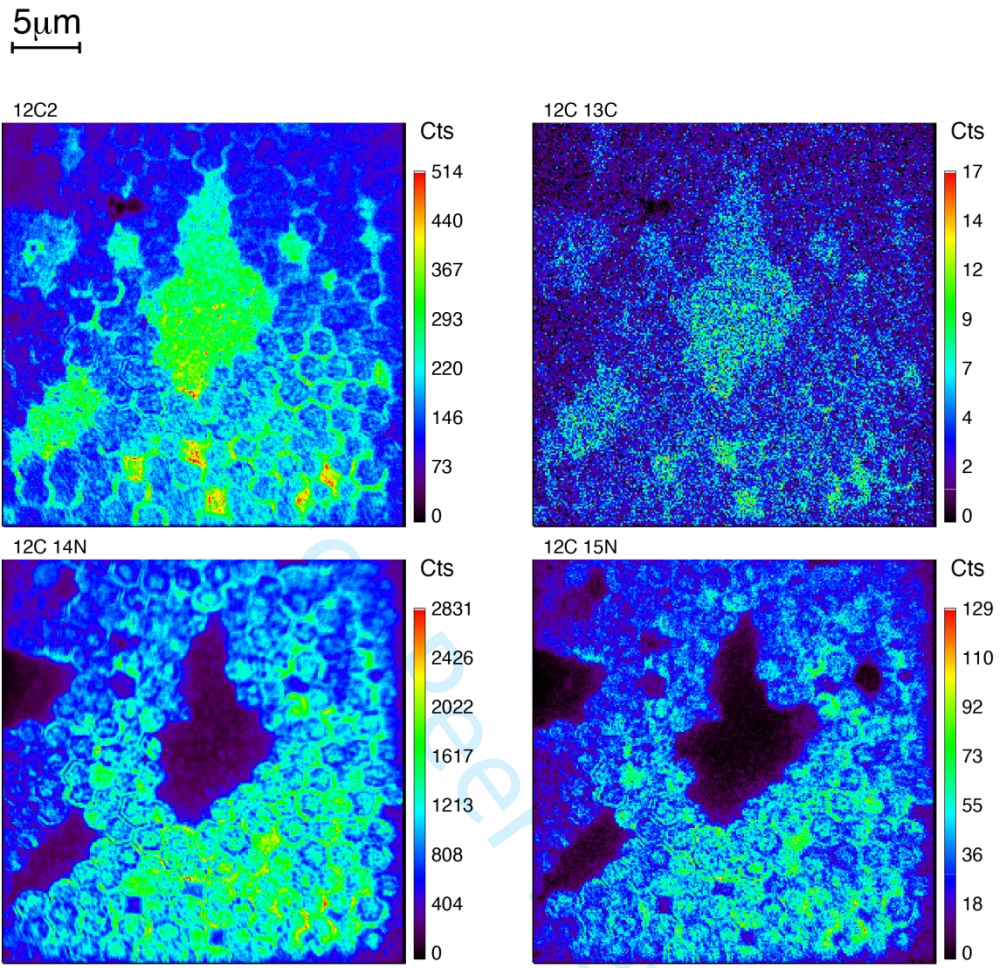


Table S1: Summary of measurements done at each repeated CTD cast in this study.

Cast number	Date (dd/mm/yyyy)	Local time (hh:mm 24 h)	qPCR counts	Microscopy counts	Bulk N ₂ fixation rates	Cell-specific N ₂ fixation rates	Amendment experiments	Organic+inorganic nutrient concentrations	dFe concentrations
018	27/03/2015	06:25					x		x
155	23/03/2015	01:00			x				
158	23/03/2015	10:10						x	
172	25/03/2015	01:05			x				
189	27/03/2015	01:06			x				
190	27/03/2015	02:48	x	x	x	x			

1
2
3 **Cited references**
4

5 Tang W, Wang S, Fonseca-Batista D *et al.* Revisiting the distribution of oceanic N₂ fixation
6 and estimating diazotrophic contribution to marine production. *Nat Commun*
7 2019;**10**:1–10.
8
9
10
11
12
13
14
15
16
17
18
19
20
21
22
23
24
25
26
27
28
29
30
31
32
33
34
35
36
37
38
39
40
41
42
43
44
45
46
47
48
49
50
51
52
53
54
55
56
57
58
59
60

For Peer Review

